Effect of the soil spatial variability on the seismic behavior of a free field elastic medium

Tamara Al-Bittar & Abdul-Hamid Soubra
University of Nantes, France

Guilhem Mollon & Daniel Dias
Joseph Fourier University, France

Pauline Billion & Nicolas Humbert
EDF-SEPTEN, France.

ABSTRACT: In this paper, the probabilistic seismic behavior of a free field elastic medium was investigated taking into account the soil spatial variability. The aim is to compute the statistical moments of the maximum acceleration at the ground surface due to a seismic acceleration time-history applied at the bottom of the free field medium. The soil shear modulus was considered as a one-dimensional non-Gaussian random field where it is assumed to vary in the vertical direction. The deterministic model was based on numerical simulations using the dynamic option of the FLAC^{3D} software. The probabilistic dynamic analyses were performed using both the classical Monte Carlo simulation (MCS) methodology and the Sparse Polynomial Chaos Expansion (SPCE) methodology.

1 INTRODUCTION

The response of a geotechnical structure subjected to a seismic loading has been extensively investigated in literature using deterministic approaches where average values of the soil properties (shear modulus, angle of internal friction, cohesion, etc.) were used. Notice however that the spatial variability of the soil properties may affect the behavior of geotechnical structures. Consequently, reliable responses of a geotechnical system cannot be predicted using a deterministic approach; a probabilistic technique seems to be necessary. The probabilistic techniques enable the rigorous propagation of the different uncertainties from the input parameters to the system responses. It should be emphasized here that few authors have worked on the analysis of the seismic responses using probabilistic approaches [e.g. Koutsourelakis et al. (2002), Nour et al. (2003), Popescu et al. (2005) and Lopez-Caballero and Modaressi-Farahmand-Rasavi (2010)]. This is because of the significant computation time required per simulation when using finite element/finite difference dynamic models.

In this paper, the effect of the soil spatial variability on the seismic responses of geotechnical structures is investigated. Given the scarcity of studies involving the probabilistic seismic responses, the case of a free field elastic soil medium subjected to a seismic loading was considered. The aim is to investigate the effect of the soil spatial variability on the maximal acceleration at the ground surface. The soil shear modulus was considered as a one-dimensional non-Gaussian random field where it is assumed to vary in the vertical direction. It was described by a square exponential autocorrelation function and was assumed to be log-normally distributed. The deterministic model was based on numerical simulations using the dynamic option of the FLAC^{3D} software. As for the probabilistic methods used in this paper, two methods were employed. The first one is the classical Monte Carlo Simulation (MCS) methodology. Because of the high computational cost of the deterministic dynamic model, a relatively small number of calls of the deterministic model was used and thus, the outcomes were only the first two statistical moments of the system response (not the failure probability). The second probabilistic method is the Sparse Polynomial Chaos Expansion (SPCE) methodology which consists in substituting the complex deterministic model by a meta-model and performing MCS on this meta-model (for the computation of the failure probability). The aim of the use of the SPCE methodology in the present paper is to check its capability to handle the probabilistic analysis of a dynamic problem. Notice finally that the main objective of the present paper is to determine the influence of the soil statistical parameters (i.e. coefficient of variation and autocorrelation distance of the soil uncertain parameter) on the statistical moments of the dynamic system response (maximum acceleration at the ground surface).

The paper is organized as follows: one first presents the deterministic numerical modeling of the

dynamic problem and the corresponding results. Then, the probabilistic analyses and the corresponding probabilistic results are presented and discussed. The paper ends by a conclusion of the main findings.

2 DETERMINISTIC ANALYSIS

In this section, the deterministic numerical model is firstly presented. It is followed by the corresponding deterministic results.

2.1 *Numerical modeling*

The deterministic model is based on numerical simulations using the dynamic option of the finite difference code FLAC^{3D}. A soil column of unit width and of 24m depth is considered for the simulation of a free field soil mass of depth equal to 24m. This is because the soil column is sufficient to simulate the propagation of the seismic waves in a homogeneous soil and to deduce the distribution of the peak acceleration as a function of depth. The input seismic signal used in this work is the synthetic signal of Nice for which the corresponding accelerogram is presented in Figure 1(a). This signal is used because it is representative of the French design spectrum [Grange (2008)]. It has a maximum acceleration equal to 0.33g. Its corresponding Fourier amplitude spectrum is shown in Figure 1(b).

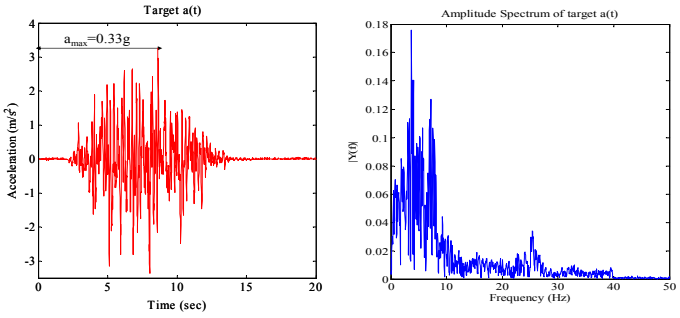

(a) (b)

Figure 1. (a) Accelerogram of the synthetic signal of Nice and (b) the corresponding Fourier amplitude spectrum

In the finite difference dynamic analysis by FLAC^{3D}, numerical distortions may occur during the propagation of the seismic waves if the elements size of the mesh is not convenient. The size Δl of an element of the mesh should respect the following condition [Itasca (2000)]:

$$\Delta l \leq \frac{V_s}{10 * f_{\max}} \tag{1}$$

where V_s is the shear wave velocity, and f_{max} is the maximum frequency of the incident seismic signal [Kuhlemeyer and Lysmer, (1973)]. The shear wave velocity V_s in Equation (1) can be calculated using the values of the soil shear modulus G and the soil density ρ as follows:

$$V_s = \sqrt{\frac{G}{\rho}} \tag{2}$$

Even though an elasto-plastic model would be more realistic to model the soil behavior especially for the cases of medium and high earthquake GMs, an elastic model was used in this work. The aim is to investigate the effect of the soil spatial variability using a simple model with a reasonable computation time. Concerning the boundary conditions, FLAC^{3D} offers the option of applying absorbing boundary conditions of type "quiet boundaries" or "free field". These boundary conditions absorb the energy of the wave approaching these limits and thus avoid the reflection of these waves. In this paper, the boundary conditions applied to the vertical boundaries are of type "free field". This type of boundary conditions is suitable for vertical surfaces while the boundary conditions of type "quiet boundaries" are generally convenient in the case of horizontal surfaces. Finally, it should be mentioned that in the natural dynamic systems, the internal friction may lead to partial dissipation of the energy of vibration. The software FLAC^{3D} provides a damping of type "Rayleigh damping" (among other types of damping) which is based on two parameters (i) the natural frequency of the system and (ii) the damping ratio (defined as a percentage of the critical damping). This type of damping is used in this paper.

2.2 *Deterministic results*

For the dynamic analyses, the values of the shear modulus, bulk modulus and density of the soil were as follows: G=100MPa, K=250MPa, and ρ=1800 kg/m^3. In order to avoid the numerical distortion that may occur during the propagation of the seismic waves in the model, the elements size must satisfy Equation (1). By using Equation (2), the shear wave velocity was found to be equal to 235.7m/s. From Figure 1(b), one can see that the maximal frequency f_{max} is equal to 40Hz. Thus, the maximum size of the different elements must be less than or equal to 0.59m. In the studied model, the size Δl of the different elements was taken equal to 0.5m. Concerning the boundary conditions, boundary conditions of type "free field" were applied along the vertical boundaries of the model. The lower horizontal boundary was subjected to the seismic load (i.e. the synthetic accelerogram of Nice). As for the parameters of the Rayleigh damping, a central frequency (natural frequency) f_c=2.5Hz and a damping ratio equal to 5% of the critical damping were used. Notice that the approximate formula of the natural frequency of a soil column given by Widmer (2003) (i.e. $f_c=V_s/4H$ where H is the height of the soil column) was employed to calculate the value of the central frequency.

Figure 2 shows the values of the maximum acceleration at the top of the soil column as a function of the shear modulus G (the range of values of G considered in this curve is that corresponding to a shear velocity varying between 200m/s and 900m/s). This curve was found (as expected) independent of the value of K because one is dealing here with only shear deformations (not volumetric deformations) induced by the seismic shear waves which dominate the strong shaking phase. From this figure, one can notice that large amplifications were obtained for the values of G that lie between $162MPa$ and $1012.5MPa$. This amplification decreases outside this range of values. In order to explain the significant values of the amplification, one should refer to the Fourier amplitude spectrum of the input seismic signal shown in Figure 1(b). From this figure, one can see that the predominant frequency band is between $3Hz$ and $9Hz$. By using the approximate formula of the natural frequency of a soil column given by Widmer (2003) (i.e. $f_c=V_s/4H$), one may show that for the values of G comprised between $162MPa$ and $1012.5MPa$, the band of predominant frequencies of the soil column coincides with the predominant frequency band of the input seismic signal. This coincidence leads to the so-called 'phenomenon of resonance' which induces the significant amplification.

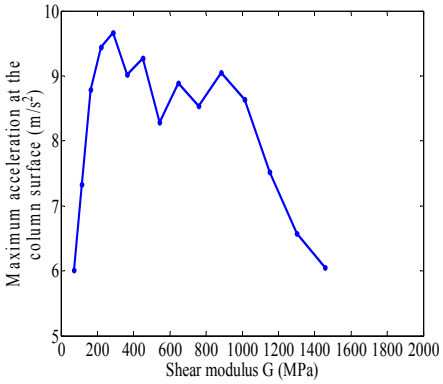

Figure 2. Maximum acceleration at the top of the column versus the shear modulus G

3 PROBABILISTIC MODELS

The aim of this section is to present the probabilistic dynamic analysis. The impact of the soil spatial variability on the dynamic response was considered. It should be remembered here that the dynamic system response involves the maximum acceleration (A_{max}) at the ground surface. The soil shear modulus G was modeled as a one-dimensional non-Gaussian random field. The EOLE methodology [Li and Der Kiureghian (1993)] was used to discretize the shear modulus random field (i.e. to obtain realizations of the soil shear modulus that respect the correlation structure of this field). For the one-dimensional random field used in this paper, the shear modulus was allowed to vary only in the vertical direction. The deterministic model was based on numerical simulations using the finite difference code FLAC^{3D}. As for the probabilistic methods used in this paper, two methods were employed. The first one is the classical crude Monte Carlo Simulation (MCS) methodology and the second one is the Sparse Polynomial Chaos Expansion (SPCE) methodology which consists in substituting the complex deterministic model by a meta-model and performing MCS on this metamodel.

In this section, the EOLE method of discretisation of random fields was firstly presented. It is followed by a brief presentation of the crude Monte Carlo method and the SPCE methodology used for the probabilistic analysis.

3.1 *Discretization of a non-isotropic log-normal random field*

Consider a 2D non-isotropic log-normal random field Z^{LN} described by: (i) a log-normal marginal cumulative distribution function F_G, and (ii) a square exponential autocorrelation function ρ_Z^{LN} [(x, y), (x', y')] which gives the values of the correlation between two arbitrary points (x, y) and (x', y'). Notice that this function is given as follows:

$$\rho_z^{LN}[(x,\ y),\ (x\ ',\ y\ ')] = \exp\left(-\left(\frac{|x-x\ '|}{a_x}\right)^2 - \left(\frac{|y-y\ '|}{a_y}\right)^2\right) \quad (3)$$

where a_x and a_y are the autocorrelation distances along x and y respectively. The EOLE method proposed by Li and Der Kiureghian (1993) to discretize a random field is used herein. In this method, one should first define a stochastic grid composed of s grid points (or nodes) and determine the log-normal autocorrelation matrix $\Sigma^{LN}_{\chi;\chi}$ which gives the correlation between each grid point of the stochastic mesh and the other grid points of this mesh using Equation (3). The log-normal autocorrelation matrix $\Sigma^{LN}_{\chi;\chi}$ should then be transformed into the Gaussian space using the Nataf transformation [cf. Nataf (1962)]. As a result, one obtains a Gaussian autocorrelation matrix $\Sigma^{G}_{\chi;\chi}$ that can be used to discretize the Gaussian random field Z as follows:

$$\tilde{Z}(x\ ,\ y\ ) \cong \mu_{\ln Z} + \sigma_{\ln Z} \sum_{j=1}^{N} \frac{\xi_j}{\sqrt{\lambda_j}}.\phi_j.\Sigma_{Z(x\ ,y\ );\chi} \quad (4)$$

where μ_{lnZ} and σ_{lnZ} are the mean and standard deviation values of the underlying normal distribution (i.e. ln(Z)); (λ_j, ϕ_j) are the eigenvalues and eigenvectors of the Gaussian autocorrelation matrix $\Sigma^{G}_{\chi;\chi}$; $\Sigma_{Z(x\ ,y\ );\chi}$ is the correlation vector between the value of the field at an arbitrary point (x, y) and its values at the different grid points; ξ_j ($j=1, \ldots, N$) is a vector of standard normal random variables; and N is the number of terms (expansion order) retained in EOLE method. This number N is obtained (i) by sorting the

eigenvalues λ_j (j=1, …, s) in a descending order and (ii) by choosing the number N of eigenmodes that leads to a variance of the error which is smaller than a prescribed tolerance ε ($\varepsilon \approx 10\%$ in this paper). Notice that the variance of the error for EOLE is given by Li and Der Kiureghian (1993) as follows:

$$Var\left[Z(x, y) - \tilde{Z}(x, y) \right] = \sigma^2_{\ln Z} \left\{ 1 - \sum_{j=1}^{N} \frac{1}{\lambda_j} \left(\left(\phi_j \right)^T \Sigma_{Z(x,y);\chi} \right)^2 \right\} \quad (5)$$

where $Z(x, y)$ and $\tilde{Z}(x, y)$ are respectively the exact and the approximate values of the random field at a given point (x, y) and $\left(\phi_j \right)^T$ is the transpose of the eigenvector ϕ_j. Once the Gaussian random field is obtained, it should be transformed into the log-normal space by exponentiating the approximated Gaussian random field $\tilde{Z}(x, y)$ given by Equation (4).

3.2 *Monte Carlo method*

The Monte Carlo simulation method consists in generating *K* samples which respect the joint probability density function $f_X(X)$ of the *M* random variables ($X_1, ..., X_M$) gathered in a vector *X*. For each sample, the system response is calculated. Thus; for the K samples, one obtains *K* values of the system response gathered in a vector $\Gamma = \left\{ \Gamma\left(X^{(1)}\right), ..., \Gamma\left(X^{(K)}\right) \right\}$ which may be used to determine (i) the estimators of the first two statistical moments of the system response and (ii) the failure probability for a prescribed threshold of this system response. A very large number of realizations is required to obtain a rigorous value of the failure probability especially when computing small failure probabilities. Notice however that a smaller number of simulations is required for the computation of the first two statistical moments of the system response.

3.3 *Sparse Polynomial Chaos Expansion (SPCE) methodology*

The polynomial chaos expansion methodology allows one to approximate a complex deterministic model by a meta-model. Thus, the system response may be calculated (when performing the probabilistic analysis by MCS) using a simple analytical equation. This method was shown in the static (non-dynamic) problems [cf. Blatman and Sudret (2010) and Mollon et al. (2011)] to provide satisfactory probabilistic results concerning not only the first two statistical moments of the system response, but also the small failure probabilities encountered in geotechnical engineering (i.e. those that lie in the range 10^{-3}-10^{-4}). Furthermore, it significantly reduces the number of calls of the deterministic model required by the crude MCS methodology (presented in the previous section) when computing a failure probability. Within the PCE methodology, the system response Γ of a model with M random variables can be expressed by a PCE (i.e. an analytical equation) as follows:

$$\Gamma_{PCE}(\xi) = \sum_{\beta=0}^{\infty} a_\beta \Psi_\beta(\xi) \cong \sum_{\beta=0}^{P-1} a_\beta \Psi_\beta(\xi) \quad (6)$$

where P is the number of terms retained in the truncation scheme, $\xi = \left\{ \xi_i \right\}_{j=1,...,M}$ is a vector of M independent standard random variables that represent the M random variables, a_β are unknown coefficients to be computed and Ψ_β are multivariate Hermite polynomials. The coefficients a_β of the PCE may be efficiently computed using a non-intrusive technique where the deterministic calculations are done using for example a finite element/finite difference software treated as a black box. The most used non-intrusive method is the regression approach (Blatman and Sudret, 2010). This method is used in the present work. It should be noticed that the number of the PCE coefficients to be computed grows dramatically with the size M of the input random vector and the PCE order p. When dealing with a random field as is the case in the present paper (and especially when considering small values of the autocorrelation distances), the discretization of the random field may lead to a significant number of random variables which makes the determination of the PCE coefficients unfeasible because of the significant increase in the number of calls of the deterministic model. To address such problem, the sparse polynomial chaos expansion methodology developed by Blatman and Sudret (2010) is used herein. Within this methodology, a truncation strategy (called the hyperbolic truncation scheme) that retains only the significant terms of the PCE is used [for more details see Blatman and Sudret (2010)]. The proposed SPCE methodology leads to a sparse polynomial chaos expansion that contains a smaller number of unknown coefficients which can be calculated from a reduced number of calls of the deterministic model. In order to achieve the numerical stability of the regression problem, the minimal number of calls of the deterministic model must be selected in such a way that the matrix of the linear system of equations of the regression problem is well conditioned. Notice also that the quality of the output approximation *via* a SPCE closely depends on the SPCE order. To ensure a good fit between the meta-model and the true deterministic model (i.e. to obtain the optimal SPCE order), one successively increases the SPCE order until a prescribed accuracy was obtained. In this paper, the coefficient of determination Q^2 is used (see Blatman and Sudret 2010). This coefficient of determination is more efficient than the classical coefficient of determination R^2 since it al-

lows one to check the capability of the meta-model of correctly predicting the model response at any point which does not belong to the experimental design.

3.4 *Probabilistic dynamic results*

The aim of this section is to study the effect of the soil spatial variability on the statistical moments of A_{max} at the top of the soil column using both the MCS and the SPCE methodologies. In both cases, the soil shear modulus G was considered as a one-dimensional (1D) non-Gaussian random field varying in the vertical direction. It was described by a square exponential autocorrelation function and was assumed to be log-normally distributed. Two reference mean values of the shear modulus were considered. The first one is $\mu_{G_1} = 72MPa$ corresponding to a non-resonant value (this value is located on the left hand part of the curve in Figure 2) and the second one is $\mu_{G_2} = 288MPa$ corresponding to a resonant value. For both cases, a coefficient of variation equal to 30% was considered as a reference value. As in the deterministic analysis, a soil column of unit width was considered. This is because in the present case, the soil exhibits spatial variability only in the vertical direction. The probabilistic dynamic results for different values of the input governing parameters are presented in the two following sections.

3.4.1 *Monte-Carlo simulation results*

In this section, the results obtained based on Monte-Carlo simulation (MCS) methodology are presented and discussed. It should be mentioned here that the number of simulations K to be used should be sufficient to accurately calculate the first two statistical moments. This number should insure the convergence of the mean estimator of A_{max} at the top of the soil column and its corresponding coefficient of variation as a function of the number of simulations. Figure 3 shows that the convergence is reached for a number of simulations larger than 300. A number of simulations K=500 was used hereafter to perform the probabilistic analysis using the MCS method.

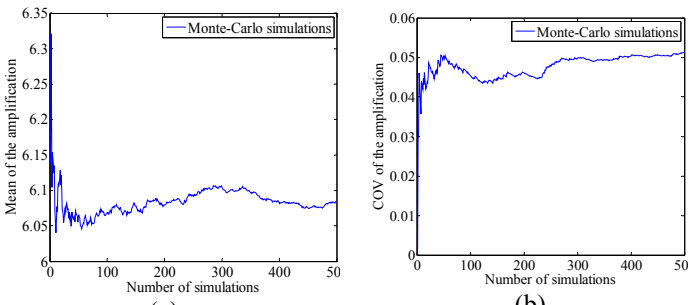

(a) (b)

Figure 3. (a) Mean and (b) coefficient of variation of A_{max} at the top of the soil column as a function of the number of simulations when a_y=0.5m

3.4.1.1 Effect of the mean value and the autocorrelation distance of the soil shear modulus

The effect of the soil spatial variability on A_{max} at the top of the soil column is studied and presented in Table 1 for the two mean values of the shear modulus ($\mu_{G_1} = 72MPa$ and $\mu_{G_2} = 288MPa$) when COV_G=30%. Different values of the vertical autocorrelation distance (a_y=0.5, 2, 5, 10 and 20m) were considered in the analyses.

Table 1 shows (as in the deterministic analysis) that smaller mean values of A_{max} at the top of the soil column were obtained when a non resonant mean value of the shear modulus G was used (i.e. $\mu_{G_1} = 72MPa$) as compared to those obtained when a resonant mean value of the shear modulus G was utilized (i.e. $\mu_{G_2} = 288MPa$). Notice also that for the weak soil configuration (i.e. when $\mu_{G_1} = 72MPa$), the mean value of A_{max} decreases when the vertical autocorrelation distance a_y decreases. This is because the increase in the soil heterogeneity will introduce further strong zones which will limit the amplification of the acceleration at the top of the soil column. On the contrary, for the strong soil configuration (i.e. $\mu_{G_2} = 288MPa$), the mean value of A_{max} increases when the vertical autocorrelation distance a_y decreases. This is because the increase in the soil heterogeneity will introduce further weakness zones which will increase the amplification of the acceleration at the top of the soil column.

On the other hand, Table 1 shows that the variability of A_{max} is maximal for the large value of the autocorrelation distance (a_y=20m). This variability decreases when the vertical autocorrelation distance a_y decreases. Indeed, the small values of the autocorrelation distance lead to a rapid change in the values of the shear modulus along the wave path. This produces quasi-similar behavior for all the realizations and leads to close values of A_{max} at the top of the soil column (and thus to a smaller variability in this response). From Table 1, one can also observe that the variability of A_{max} is larger for the case of the weak soil corresponding to a small mean value of the shear modulus G (i.e. $\mu_{G_1} = 72MPa$).

Table 1. Effect of the soil spatial variability on the maximum acceleration at the top of the soil column as obtained from MCS

	$\mu_{G_1} = 72MPa$			$\mu_{G_2} = 288MPa$		
a_y (m)	μ_{Amax} (m/s^2)	σ_{Amax} (m/s^2)	COV_{Amax} (%)	μ_{Amax} (m/s^2)	σ_{Amax} (m/s^2)	COV_{Amax} (%)
0.5	6.08	0.31	5.12	9.82	0.19	1.92
2	6.19	0.43	6.96	9.76	0.30	3.95
5	6.29	0.54	8.52	9.65	0.49	5.03
10	6.35	0.66	10.34	9.60	0.55	5.75
20	6.38	0.66	10.34	9.53	0.55	5.80

3.4.1.2 Effect of the coefficient of variation of the soil shear modulus

The aim of this section is to study the effect of the coefficient of variation of G on the statistical moments of A_{max} at the top of the soil column for the two mean values of G ($\mu_{G_1} = 72MPa$ and $\mu_{G_2} = 288MPa$).

Table 2 shows that the increase in the coefficient of variation of G has practically no influence on the mean value of A_{max}. On the other hand, the variability of A_{max} at the top of the column increases (as expected) when the coefficient of variation of G increases. Finally, notice that the variability of A_{max} at the top of the column reaches the most significant values in the case of a weak soil ($\mu_{G_1} = 72MPa$).

Table 2. Effect of the coefficient of variation of G on A_{max} at the top of the soil column as obtained from MCS

	$\mu_{G_1} = 72MPa$			$\mu_{G_2} = 288MPa$		
COV_G (%)	μ_{Amax} (m/s^2)	σ_{Amax} (m/s^2)	COV_{Amax} (%)	μ_{Amax} (m/s^2)	σ_{Amax} (m/s^2)	COV_{Amax} (%)
15	6.13	0.41	6.61	9.74	0.17	1.78
30	6.19	0.43	6.96	9.65	0.49	5.03
45	6.16	0.52	8.42	9.60	0.64	6.70

3.4.2 *Sparse polynomial chaos expansion results*

In this section, the results obtained based on the sparse polynomial chaos expansion (SPCE) methodology are presented. It should be mentioned here that the 500 simulations which were used in the previous section to perform the analyses by the MCS methodology were employed herein in order to construct the SPCE. Additional simulations were performed for the cases where the regression problem was ill-posed. However, the number of simulations was not increased until reaching the target coefficient of determination Q^2_{TARGET} of 0.999. This is because of the high computational cost of the dynamic analysis.

3.4.2.1 Effect of the mean value and the autocorrelation distance

The effect of the soil spatial variability on the PDF of A_{max} at the top of the soil column for the two mean values of the shear modulus ($\mu_{G_1} = 72MPa$ and $\mu_{G_2} = 288MPa$) is studied and presented in Figure 4. This figure shows that the variability of A_{max} at the top of the soil column decreases when the vertical autocorrelation distance a_y decreases. Similar observation was provided in a previous section where MCS was employed. Even though these PDFs present logical trends, they cannot be considered as rigorous. This is because relatively small values of the coefficient of determination Q^2 were obtained in this case where a seismic loading was considered.

Table 3 presents a comparison between the statistical moments of A_{max} at the top of the soil column as obtained by MCS and by the SPCE methodology. This table also provides the values of Q^2 obtained when the SPCE methodology was used. From Table 3, one can observe a small difference between the first two statistical moments as given by the MCS and the SPCE methodologies even though relatively small values of Q^2 were obtained with the use of the SPCE methodology. Thus, the relatively small values of Q^2 may not have a major influence on the two first statistical moments, but they certainly affect the third and fourth statistical moments. This makes the obtained PDFs invalid at the distribution tails.

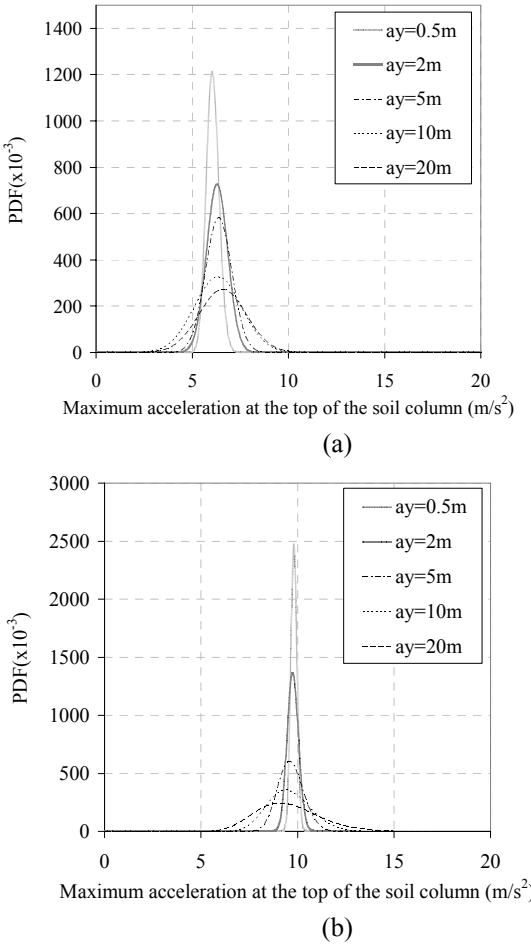

Figure 4. Influence of the vertical autocorrelation distance a_y on the PDF of A_{max} at the top of the soil column (as obtained from the SPCE methodology) when (a) $\mu_{G_1} = 72MPa$ and (b) $\mu_{G_2} = 288MPa$

In fact, there are two possible reasons for which relatively small values of Q^2 may occur. The first one is the chosen system response (i.e. A_{max}) which may be obtained at different time steps from simulation to another one. As for the second reason, it may be the number of simulations which needs to be increased.

In order to detect the main reason for which the relatively small values of Q^2 were obtained, a test on only the chosen system response A_{max} was performed. This test is presented in Appendix A. It was found that the chosen system response is not the reason why one obtains small values of Q^2. As for the number of simulations, the test was not performed because of the significant computation time of the dynamic deterministic model (40 min per simulation). As a conclusion, more advanced probabilistic

methods are needed in the presence of seismic loading where highly non-linear models are involved.

Table 3. Comparison between the statistical moments (μ, σ) of A_{max} at the top of the soil column as obtained by MCS and by the SPCE methodology

$\mu_{G_1} = 72MPa$							
	Monte-Carlo simulations			Sparse Polynomial Chaos Expansion			
a_y (m)	μ_{Amax} (m/s^2)	σ_{Amax} (m/s^2)	COV_{Amax} (%)	μ_{Amax} (m/s^2)	σ_{Amax} (m/s^2)	COV_{Amax} (%)	Q^2
0.5	6.08	0.31	5.12	6.07	0.23	3.97	0.535
2	6.19	0.43	6.96	6.18	0.37	6.00	0.587
5	6.29	0.53	8.52	6.29	0.42	6.68	0.686
10	6.35	0.65	10.34	6.33	0.54	8.53	0.788
20	6.38	0.66	10.34	6.37	0.56	8.80	0.790
$\mu_{G_2} = 288MPa$							
	Monte-Carlo simulations			Sparse Polynomial Chaos Expansion			
a_y (m)	μ_{Amax} (m/s^2)	σ_{Amax} (m/s^2)	COV_{Amax} (%)	μ_{Amax} (m/s^2)	σ_{Amax} (m/s^2)	COV_{Amax} (%)	Q^2
0.5	9.82	0.19	1.92	9.81	0.14	1.43	0.555
2	9.76	0.30	3.95	9.76	0.27	2.77	0.665
5	9.65	0.49	5.03	9.65	0.46	4.77	0.810
10	9.60	0.55	5.75	9.60	0.50	5.21	0.800
20	9.53	0.55	5.80	9.53	0.50	5.25	0.750

4 CONCLUSION

In this paper, the dynamic response induced by a seismic loading taking into account the soil spatial variability was investigated. Given the scarcity of studies involving the probabilistic seismic responses, a free field elastic soil medium subjected to a seismic loading was considered. The aim is to investigate the effect of the soil spatial variability on the maximal acceleration at the ground surface using a simple model with a reasonable computation time.

The soil shear modulus G was modeled as a non-Gaussian random field. The EOLE methodology was used to discretize the shear modulus random field. The deterministic dynamic numerical model was based on numerical simulations using the dynamic option of the finite difference software FLAC^{3D}. As for the probabilistic methods used in this paper, two methods were employed. The first one is the classical Monte Carlo Simulation (MCS) methodology and the second one is the Sparse Polynomial Chaos Expansion (SPCE) methodology which consists in substituting the original deterministic model by a meta-model and performing MCS on this metamodel.

In the framework of the deterministic analysis, the evolution of the maximum acceleration as a function of the shear modulus have shown that for a given range of values of the shear modulus, an important increase in the maximum acceleration was obtained. For this range of values of G, the predominant frequency band of the soil 'column' corresponds to the predominant frequency band of the seismic loading, which leads to the so-called resonance phenomenon.

The MCS methodology has shown that for the Nice accelerogram used in this paper, smaller mean values of A_{max} at the top of the soil column were obtained when a non-resonant mean value of the shear modulus G was used (i.e. $\mu_{G_1} = 72MPa$) as compared to those obtained when a resonant mean value of the shear modulus G was utilized (i.e. $\mu_{G_2} = 288MPa$). On the other hand, the variability of A_{max} is maximal for the very large values of the autocorrelation distance. This variability decreases when the vertical autocorrelation distance a_y decreases. As for the results obtained from the SPCE methodology, the statistical moments of A_{max} at the top of the soil column are close to those resulting from the MCS methodology, but the obtained PDFs can not be considered as rigorous because relatively small values of Q^2 were obtained. As a conclusion, more advanced probabilistic methods are needed in the presence of seismic loading where highly non-linear models are involved.

REFERENCES

Al-Bittar, T. and Soubra, A. H. Bearing capacity of strip footing on spatially random soils using sparse polynomial chaos expansion. *International Journal for Numerical and Analytical Methods in Geomechanics*, accepted paper, 2012.

Blatman, G. and Sudret, B. An adaptive algorithm to build up sparse polynomial chaos expansions for stochastic finite element analysis. *Probabilistic Engineering Mechanics*, 25: 183-197, 2010.

Blatman, G., and Sudret, B. Principal component analysis and Least Angle Regression in spectral stochastic finite element analysis. *Applications of Statistics and Probability in Civil Engineering*. 669-676, 2011.

Grange, S. Risque sismique: stratégie de modélisation pour simuler la réponse des structures en béton et leurs interactions avec le sol. *Ph.D thesis*, INPG, 2008.

Itasca. FLAC 4.0 Manuals. – Minnesota, ITASCA Consulting Group, Inc 2000.

Koutsourelakis, S., Prevost, J.H., and Deodatis, G. Risk assessement of an interacting structure-soil system due to liquefaction. *Earthquake Engineering and Structural Dynamic*, 31: 851-879, 2002.

Kuhlemeyer, R. L., and Lysmer, J. Finite element method accuracy for wave propagation problems. *Journal of Soil Mechanics & Foundations*, 99: 421-427, 1973.

Li, C.C., and Der Kiureghian, A. Optimal discretization of random fields. *Journal of Engineering Mechanics*, 119(6): 1136-1154, 1993.

Lopez-Caballero, F., and Modaressi Farahmand-Razavi,A. Assessment of variability and uncertainties effects on the seismic response of a liquefiable soil profile. *Soil Dynamics and Earthquake Engineering*, 30(7): 600-613, 2010.

Mollon, G., Dias, D., and Soubra, A.-H. Probabilistic analysis of pressurized tunnels against face stability using collocation-based stochastic response surface method. *Journal of Geotechnical and Geoenvironmental Engineering*, *ASCE,* 137(4): 385-397, 2011.

Nataf, A. Détermination des distributions de probabilités dont les marges sont données. *CR Acad Sci*, 225: 42-3, 1962.

Nour, A., Slimania, A., Laouamia, N., and Afraa, H. Finite element model for the probabilistic seismic response of heterogeneous soil profile. *Soil Dynamics and Earthquake Engineering*, 23: 331-348, 2003.

Popescu, R., Prevost, J.H., and Deodatis, G. 3D effects in seismic liquefaction of stochastically variable soil deposits. *Géotechnique*, 55(1): 21-31, 2005.

Widmer, F., Duvernay, B., Fäh, D., and Parriaux, A. Projet pilote de microzonage sismique à Yverdon (VD). *Bulletin for Applied Geology*, 8: 5-16, 2003.

Appendix A

The purpose of this Appendix is to check if the possible reason for which relatively small values of Q^2 were obtained (when the SPCE methodology was applied) is linked to the chosen system response (i.e. A_{max}). Notice that the test was performed when $\mu_{G_1} = 72MPa$ and a_y=2m.

The test consists in constructing the SPCE not only for A_{max} at the top of the soil column but for all the accelerations at the top of the soil column at the different time steps (the value of A_{max} can be deduced from the different SPCEs constructed at the different time steps). This test allows one to detect if the fact of considering directly A_{max} as a system response is the reason for which the relatively small values of Q^2 were obtained.

Notice that a seismic loading of total duration T=15s and time step Δt=0.05s was considered in the analysis. Thus, it is composed of 301 registration points (or acceleration values). The construction of the SPCE 301 times is a difficult task. Blatman and Sudret (2011) have suggested an efficient and fast alternative approach. To obtain the SPCEs for all the accelerations at the different time steps, Blatman and Sudret (2011) have proposed the use of the so-called *principal component analysis* (PCA). The aim is to capture the main stochastic feature of the response using a small number of (non physical) variables compared to the original number of variables (i.e. 301 in the present analysis). This enormously reduces the computational cost since the SPCEs are no longer evaluated for all the accelerations at the different time steps, but on a small number of non physical variables. The SPCEs computed for the non-physical variables are then used to deduce the SPCEs for all the accelerations at the different time steps. The *principal component analysis* (PCA) was detailed in Blatman and Sudret (2011) and was not presented herein.

In this section, one presents the numerical results obtained using the PCA which was previously presented. For the 301 registration points, only five SPCEs were found necessary to estimate the SPCEs of the 301 registration points. Notice that the values of Q^2 obtained for the five most influent eigenmodes (when using the 500 MC simulations) were respectively 0.65, 0.6, 0.2, 0.2 and 0.2.

Table A.1 presents the first two statistical moments as obtained from the direct determination of the SPCEs at three different arbitrary times (t_1=2.5s, t_2=5s and t_3=10s). In the same table, one also presents the first two statistical moments as obtained from the SPCEs deduced after performing a PCA on the output matrix Γ. This table shows that the presented results using the PCA are in good agreement with those obtained form the direct determination of the SPCE at the three chosen times. Even though satisfactory results for the first two statistical moments were obtained, unsatisfactory values of Q^2 were obtained when using either the PCA or the direct determination of the SPCE. Thus, for such types of problems, one needs to find more advanced stochastic models in order to obtain more rigorous meta-models for the highly non-linear problems.

Table A.1. Values of the first two statistical moments and the coefficient of determination Q^2

	Direct determination of the SPCEs			Determination of the SPCEs using the PCA	
	μ_A (m/s^2)	σ_A (m/s^2)	Q^2	μ_A (m/s^2)	σ_A (m/s^2)
t_1=2.5s	0	0.80	0.66	-0.05	0.71
t_2=5s	-1.58	3.33	0.81	-1.52	3.82
t_3=10s	0.9	2.67	0.69	0.87	2.90